The Anticodon-binding Domain of Tyrosyl-tRNA Synthetase: State of Folding and Origin of the Crystallographic Disorder

Valérie Guez,[‡] Shamila Nair,[§] Alain Chaffotte,[‡] and Hugues Bedouelle*,[‡]

Unité de Biochimie Cellulaire, CNRS-URA1129, Institut Pasteur, 28 rue du Docteur Roux, 75724 Paris Cedex 15, France, and Faculté de Médecine Necker, INSERM-U411, 156 Rue de Vaugirard, 75730 Paris Cedex 15, France

Received October 13, 1999; Revised Manuscript Received December 1, 1999

ABSTRACT: The C-terminal domain (residues 320−419) of tyrosyl-tRNA synthetase (TyrRS) from *Bacillus stearothermophilus* is disordered in the crystal structure. Its function consists of binding the anticodon of $tRNA^{Tyr}$. We undertook to characterize its conformational state. A hybrid between the C-terminal fragment and a His-tag sequence was constructed and purified in large amounts. Analyses by mass spectrometry and analytical ultracentrifugation showed that the C-terminal fragment, thus purified, was not degraded and that it neither dimerized nor aggregated. Its far- and near-UV circular dichroism spectra revealed a high content in secondary structures and an asymmetrical environment of its aromatic residues. Each spectrum could be reconstructed by the difference between the corresponding spectra for the full-length TyrRS and for its N-terminal fragment. The Stokes radius of the C-terminal fragment, measured by size exclusion chromatography, indicated a condensed globular state. The fluorescence of ANS (a small hydrophobic probe) showed that the surface of the C-terminal fragment was more hydrophilic than that of a molten globule. These results on the C-terminal fragment and our previous observations that it can undergo cooperative transitions, demonstrated the following points: it is not in a disordered or molten globular state, it has a defined and stable three-dimensional structure, its structures are similar in its isolated and integrated forms, and the apparent disorder in the crystals of the full-length synthetase must be due to the flexibility of the polypeptide segment that links the N- and C-terminal domains. Thus, TyrRS has not evolved strong noncovalent interactions between its catalytic and anticodon-binding domains, contrary to the other synthetases.

Tyrosyl-tRNA synthetase (TyrRS)[1] is a homodimeric protein, which catalyses the charging of $tRNA^{Tyr}$ in a two-step reaction. Tyrosine is first activated with ATP to give tyrosyl adenylate (Tyr-AMP), then transferred to the acceptor end of the tRNA. The crystal structure of TyrRS from *Bacillus stearothermophilus* has been solved at 2.3 Å resolution. It shows that each subunit comprises two sequential structural domains. The N-terminal domain (residues 1−319) is well-ordered. It contains the binding site for Tyr-AMP and the interface of dimerization. Within the crystals, the N-terminal domains of adjacent molecules pack tighly together to form layers that have a maximal thickness of 60 Å and are separated by gaps of 20 Å. The C-terminal domain (residues 320−419) occupies the gaps between these layers, but its electron density is too weak for one to trace the polypeptide chain. Difference maps show a continuous volume of electron density, approximately 1500 $Å^3$, which might correspond to part of the C-terminal domain but does not reveal any defined structure (*1*). The C-terminal domain from *B. stearothermophilus* has, therefore, been considered as disordered and its sequence has been included in the training set of neural network algorithms that predict disordered segments in proteins (*1*−*3*).

The apparent disorder of the C-terminal domain in the crystal structure of TyrRS could be due to one of the following causes. It could be in an unfolded state or in an unfinished folding state in the absence of $tRNA^{Tyr}$, and its conformation could fluctuate permanently in the crystals. It could adopt several different structures, which would coexist in the crystals and would be stabilized by intermolecular contacts. Finally, it could have a single and defined structure but adopt several orientations with respect to the N-terminal domain in the crystals, due to the flexibility of the polypeptide that links them.

We have previously reported that the isolated form of the C-terminal domain (C-terminal fragment) undergoes cooperative conformational transitions when treated with heat or urea, that it is in a condensed state and that a high proportion of its residues belong to secondary structure elements. These results have shown that the C-terminal domain of TyrRS is at least partially folded (*4*). A wide diversity of condensed states have been described for polypeptides, ranging from the premolten globule, which is highly dynamic and may not resemble the native structure, to the canonical molten globule that shows nativelike secondary and supersecondary structures, then to the compact, well-defined, native structure of globular proteins (*5*−*7*). We, therefore, undertook to

* To whom correspondence should be addressed. Telephone: 33 1 45 68 83 79. Fax: 33 1 40 61 30 43. E-mail: hbedouel@pasteur.fr.

‡ Unité de Biochimie Cellulaire.

§ Faculté de Médecine Necker.

[1] Abbreviations used: amu, atomic mass unit; ANS, 8-anilino-1-naphthalene sulfonic acid; aaRS, aminoacyl-tRNA synthetase; CD, circular dichroism; IPTG, isopropyl-β-D-thiogalacto-pyranoside; MALDI-TOF, matrix-assisted laser desorption ionisation time-of-flight; M_r, relative molecular mass; NMR, nuclear magnetic resonance; TyrRS, tyrosyl-tRNA synthetase.

10.1021/bi992382v CCC: $19.00
Published on Web 01/26/2000

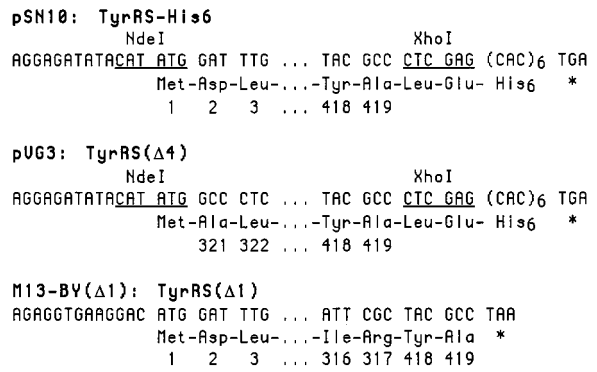

FIGURE 1: Sequences of the *tyrS* gene derivatives used in this study. The amino acid sequence of the wild-type TyrRS, at the junction between the N- and C-terminal domains is: Ile316-Arg317-Ile318-Ser319-Glu320-Ala321-Leu322. The sequences of the *tyrS* gene, of the *tyrS(Δ1)* allele, and of their 5′ regions have been reported (*36*, *62*, *63*).

further characterize the conformational state of the C-terminal fragment, to identify which of these condensed states it adopts.

In this study, we report the construction of an *Escherichia coli* strain that overproduces a recombinant form of the C-terminal fragment, its purification, and the values of several physical parameters that are usually used to characterize the molten globular state of proteins: the Stokes radius, to measure their compactness; the binding of the hydrophobic fluorescent compound 8-anilino-1-naphthalene sulfonic acid (ANS), to probe the accessibility of their hydrophobic core; the spectrum of circular dichroism (CD) in the far-UV region, to quantify the amount of residues in secondary structures; the CD spectrum in the near-UV, to characterize the mobility of the aromatic side-chains. The results will be discussed in terms of order vs disorder within the C-terminal domain of TyrRS and compared with the crystal structures of 14 other aminoacyl-tRNA synthetases.

MATERIALS AND METHODS

Parental Bacterial Strains, Plasmids, and Phages. The *E. coli* strains TG2, JM109, BL21, BL21(DE3) (*8*), and HB2200 (*9*), plasmids pET20b(+) (www.novagen.com) and pBR322-BY(M24) (*10*), and phages M13-BY(BsmI) (*11*) and M13-BY(Δ1) (*12*) have been described. pBR322-BY(M24) carries the wild-type *tyrS* gene from *B. stearothermophilus*, coding for TyrRS. M13-BY(*Bsm*I) carries the mutant allele *tyrS-(Bsm*I*)*, in which the mutant codon TCG (Cys) replaces the wild-type codon GCG (Ala) in position 321 and introduces a *Bsm*I restriction site. M13-BY(Δ1) codes for the N-terminal fragment of TyrRS (Figure 1). pET20b(+) is an expression vector in which the transcription of the cloned gene is under control of a phage T7-promoter. Strain BL21(DE3) was used for the expression of the genes cloned into pET20b(+).

Media and Buffers. The LB and 2YT culture media have been described (*8*). The concentrations of ampicillin and IPTG used were 100 μg/mL and 0.2 mM, respectively. The following buffers were used: buffer A, 20 mM Tris-Cl, pH 7.9, 0.5 M NaCl; buffer B, 20 mM K_2HPO_4/KH_2PO_4, pH 6.8; buffer C, 50 mM Na_2HPO_4/NaH_2PO_4, pH 7.0, 0.2 M NaCl.

Plasmid Constructions. The *tyrS* gene from *B. stearothermophilus* was amplified from plasmid pBR322-BY(M24) via PCR using the following oligonucleotides as primers: 5′-GTTTATCGTACA*CATATG*GATTTGCTTGCGG-AATTGCAATGGCGC-3′ and 5′-GTTATTCTA*CTCGAG*-GGCGTAGCGAATCAAATAATACTTTTT-3′. The amplified DNA fragment was inserted between the *Nde*I and *Xho*I sites (italicized in the primers) of plasmid pET20b(+) to yield pSN10 (Figure 1). In plasmid pSN10, the 3′ end of the *tyrS* gene is fused with a DNA segment, which codes for N-Leu-Glu-$(His)_6$-C. We called the hybrid gene *tyrS*(His6) and its product TyrRS−His6. Plasmid pVG3, a derivative of pSN10 in which codons 2−320 of the *tyrS*(His6) gene are deleted, was constructed in three steps. We first introduced the *Bsm*I restriction site, which is present in the *tyrS(Bsm*I*)* allele at codon positions 320−321, into the *tyrS*(His6) allele. The introduction of the *Bsm*I site was done by transferring the restriction fragment that is located between the *BsiW*I site (codon 248) and the *Sac*II site (codon 377) of the *tyrS* gene, from the DNA of phage M13-BY(*Bsm*I) into the DNA of plasmid pSN10. The resulting plasmid was called pVG1. We then introduced a DNA adapter, coding for a *Nde*I restriction site, into the *Bsm*I site of pVG1. This adaptor was formed by hybrization of two complementary oligonucleotides, 5′-ATATGGCCC-3′ and 5′-GCCATATGG-3′. The resulting plasmid was called pVG2. We finally deleted the restriction fragment that was located between the two *Nde*I sites of pVG2 to give plasmid pVG3. The resulting allele of the *tyrS* gene, carried by pVG3, was called *tyrS(*Δ4). It codes for a hybrid protein, TyrRS(Δ4), between a C-terminal fragment of TyrRS and the octapeptide N-Leu-Gly-His_6-C (Figure 1). The integrity of the full *tyrS*(His6) allele and of its flanking regions, carried by pSN10, and that of the *BsiW*I−*Sac*II fragment of the *tyrS(Bsm*I*)* allele, carried by M13-BY(*Bsm*I), were verified by DNA sequencing as described (*13*).

Protein Production and Purification. For the production and purification of TyrRS−His6 or TyrRS(Δ4), strain BL21-(DE3, pSN10) or BL21(DE3, pVG3) was grown in 100 mL of 2YT broth, supplemented with ampicillin, at 37 °C until $A_{600nm} = 2.0$. IPTG was then added to induce the expression of the TyrRS derivatives and the bacterial growth was continued until $A_{600nm} = 3.0$ (approximately 3 h). The culture was centrifuged (30 min, 4 °C, 4000 rpm), and the cell pellet was resuspended in 10 mL of binding buffer (5 mM imidazole in buffer A). The cell suspension was sonicated 3 times for 1 min each (Branson sonicator, 1 cm diameter probe). The cell debris were removed by centrifugation (30 min, 4 °C, 13000 rpm). The soluble extract was filtered through a 0.45 μm pore filter (Millipore) and purified immediately on a column of nickel chelation resin (2.5 mL), as prescribed by the manufacturer (Novagen) but with the following modifications. After the column was loaded with the sample, the column was washed with 10 volumes of binding buffer, then with 6 volumes of 20 mM imidazole in buffer A. The protein was eluted with 60 mM imidazole in buffer A, in 2 mL fractions. The content of each fraction was analyzed by electrophoresis through SDS-PAGE polyacrylamide gels, stained with Coomassie blue. The pure fractions were pooled, and the protein was concentrated up to 1 mM with a Centricon 30 (Amicon) for TyrRS−His6, or a Centricon 10 for TyrRS(Δ4). TyrRS(Δ1) was overexpressed from phage M13-BY(Δ1) and purified as described (*4*, *1*). The purified proteins were dialyzed against buffer B for TyrRS−His6 and TyrRS(Δ4), or against 20 mM Tris-HCl, pH 7.78,

5 mM 2-mercaptoethanol for TyrRS(Δ1), snap frozen in liquid nitrogen, and kept at −70 °C. The concentration of acrylamide (acrylamide/bisacrylamide = 29:1) in the gels was 8% for TyrRS−His6 and TyrRS(Δ1), and 17% for TyrRS(Δ4).

Protein Concentration. We determined the extinction coefficients of the TyrRS derivatives from the absorbance and amino acid analysis of purified samples. A purified preparation of protein was dialyzed against buffer B. Its absorption spectrum was recorded in a double-beam spectrophotometer (Perkin-Elmer) using the dialysis buffer as a blank. A sample of the protein preparation was hydrolyzed in 6 N HCl, 0.2% phenol at 110 °C for 20 h in a sealed tube. Norleucine was added as an internal standard to the sample before hydrolysis. An aliquot of the hydrolysate was analyzed on a Beckman 6300 amino acid analyzer. Occasionally, the concentration of protein was measured with the Bio-Rad Protein Assay Kit, using bovine serum albumin as a standard. The number of residues and predicted molecular masses (M_r) of the monomers are: 427 residues and 48 367 for TyrRS−His6; 319 residues and 36 324 for TyrRS(Δ1); 107 residues and 11 980.4 for TyrRS(Δ4), respectively (Figure 1).

Activity Assays. The active-site titrations and tRNA charging assays were performed as described (*12*). The charging capacity of pure *E. coli* $tRNA^{Tyr}$ (Boehringer-Manheim) was determined using 100 nM purified TyrRS−His6 and was equal to 980 pmol/A_{260nm} unit. We used a concentration of TyrRS−His6 equal to 0.5 nM and varied the concentration of $tRNA^{Tyr}$ between 0.1 and 6.3 μM for the determination of the kinetic parameters k_{cat} and K_M.

Mass Spectrometry. The spectrum of positive ions was recorded in linear mode with a MALDI-TOF mass spectrometer (Voyager Elite, Perseptive Biosystem Inc., Framingham, MA) using a saturated solution of sinapinic acid (3,5-dimethoxy-4-hydroxycinnamic acid, Aldrich) in 30% acetonitrile, 0.1% aqueous trifluoroacetic acid, as a matrix. A nitrogen laser beam (λ = 337 nm) was used for desorption. Typically, 150−256 shots were averaged for each acquired spectrum. Calibration, either internal or external, was performed with a mixture of apomyoglobin and thioredoxin using the monoprotonated ion of the monomers with average mass-to-charge (m/z) ratios corresponding to 16 952.5 and 11 674.48 amu, respectively. Before analysis, the protein sample was dialyzed against 20 mM Tris-HCl, pH 7.78, and diluted to 4 pmol/mL in 0.1% aqueous trifluoroacetic acid. It was then mixed 1:1 with the MALDI matrix.

Analytical Ultracentrifugation. We used a XLA centrifuge (Beckman) with 12 mm path-length cells. The cells were scanned at A_{280nm} to determine the distribution of protein, and at A_{350nm}, a wavelength at which the proteins do not absorb, to determine the optical baseline. The data from three successive scans were averaged. The protein (140 μL, 0.8 mg/mL), previously dialyzed against buffer B, and buffer B (150 μL) were layered over a cushion of FC43 fluorocarbon (50 μL, 3 M) in the sample sector and in the reference sector, respectively. The comparison of successive scans, made at 2 h intervals, showed that the equilibrium of sedimentation−diffusion was reached after 23 h of centrifugation at 35 000 rpm, 20 °C. We used the software provided with the XLA centrifuge to analyze the data, recorded at equilibrium. Three different theoretical models were tried: (1) an ideal solution with one solute molecule, (2) an ideal solution with two solute molecules, (3) an equilibrium of association−dissociation between monomers, dimers, trimers, and tetramers, with M_r = 11 980 for the monomer.

Size-exclusion Chromatography (SEC). We used a Superdex 75 HR10/30 column, coupled to a FPLC system (Pharmacia), and monitored its effluent with A_{280nm}. The column was equilibrated and all the chromatographic runs were performed with buffer C, at a flow rate of 0.5 mL/min and room temperature (22−26 °C). The protein samples were prepared in the same buffer. The column was calibrated with acetone for the total volume (V_t = 20.05 mL), calf thymus DNA for the void volume (V_o = 7.15 mL), horse heart cytochrome *c* (Sigma), hen egg-white lysozyme (Boehringer), bovine serum albumin (Biorad), milk β-lactoglobulin (Sigma), pancreatic ribonuclease (Pharmacia), and chymotrypsinogen (Sigma). The R_S values of these proteins have been determined previously in the same buffer conditions (*14*) or calculated from their diffusion coefficients (*15*). The R_S values of the calibration proteins and their partition coefficients $K_{av} = (V_e - V_o)/(V_t - V_o)$ where V_e is the elution volume, followed the relation $K_{av} = 0.85 \pm 0.07 - (0.017 \pm 0.003) \times R_S$. The K_{av} value of TyrRS(Δ4) was determined from 3 independent runs.

ANS-binding. The fluorescence emission spectra of ANS were recorded with a LS5B spectrofluorometer (Perkin-Elmer), an excitation wavelength of 370 nm and 2.5 nm bandwidth for both excitation and emission. The spectra of ANS in mixtures of ethanol and water were recorded as described (*16*).

Circular Dichroism. The CD spectra were recorded with a CD6 spectropolarimeter (Jobin-Yvon, Longjumeau, France), with a step of 0.5 nm and an integration time of 2 s. Each spectrum was obtained by averaging 5 successive acquisitions. The buffer baseline was acquired under the same conditions and then subtracted from the sample spectrum. The resulting spectra were expressed as molar ellipticities in the near UV region and as molar ellipticities/residue in the far-UV. The content of TyrRS(Δ4) in secondary structures was predicted with the Varselec program and a database of 33 proteins (*17*, *18*). Trypsin and γ-cristallin were removed from the database to improve the prediction; the sum of the fractional structural types was then equal to 1.04 and the root-mean-square error to 0.149. Spectra were recorded for TyrRS−His6, TyrRS(Δ1) and TyrRS(Δ4) at approximately identical concentrations. The spectrum for TyrRS(Δ4) was reconstructed from those of TyrRS−His6 and TyrRS(Δ1) by writing that the ellipticity for TyrRS(Δ4) was a linear combination of those for TyrRS−His6 and TyrRS(Δ1). The linearity coefficients were calculated at two wavelengths, 193.5 and 209.0 nm in the far-UV region, and 258.5 and 277.5 nm in the near-UV region, corresponding to the minimal and maximal ellipticities of TyrRS−His6.

RESULTS

Production and Purification of TyrRS−His6 and Its C-terminal Fragment. We constructed two new recombinant plasmids, which were derived from an expression vector of the pET series (*19*) to produce and purify TyrRS from *B. stearothermophilus* and its C-terminal fragment in high quantities. Plasmid pSN10 carried a hybrid gene between

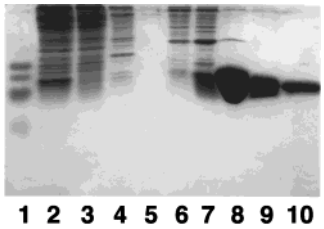

FIGURE 2: Purification of TyrRS(Δ4) by affinity chromatography on immobilized Ni^{2+}. The fractions were analyzed by electrophoresis through 17% SDS-polyacrylamide gels. The proteins were stained with Coomassie blue. Lane 1, marker proteins with M_r equal to 16 900, 14 400, and 8200; lane 2, soluble extract; lane 3: fraction flowing through the resin; lane 4, fractions of washing with 20 mM imidazole; lanes 5−10, fractions of elution (2 mL each) with 60 mM imidazole. The fractions containing the pure protein (lanes 8, 9, and 10) were pooled.

tyrS (codons 1−419), which codes for TyrRS, and a 3′-terminal extension of 24 nucleotides, which coded for the octapeptide N-Leu-Glu-His_6-C (His-tag), under control of a promoter for the RNA polymerase of phage T7. Plasmid pVG3 was a derivative of pSN10 in which codons 2−320 of the *tyrS* gene were deleted (Figure 1). Therefore, it coded for a C-terminal fragment of TyrRS. The proteins coded by plasmids pSN10 and pVG3 were called TyrRS−His6 and TyrRS(Δ4) to distinguish them from previous constructions. The productions of TyrRS−His6 and TyrRS(Δ4) from plasmids pSN10 and pVG3 were not toxic for the host strain BL21(DE3). Both proteins were purified by chromatography on nickel columns. The purified TyrRS−His6 and TyrRS(Δ4) were homogeneous at more than 98% and had the expected electrophoretic mobilities, which indicated that they were not proteolyzed (Figure 2). We routinely obtained 21 mg of pure TyrRS−His6 and 13 mg of pure TyrRS(Δ4) from 100 mL of bacterial cultures.

Authenticity of TyrRS−His6 and Its C-terminal Fragment. The authenticity of the genes coding for TyrRS−His6 and for its C-terminal fragment TyrRS(Δ4) were verified by DNA sequencing. The compositions in amino acids of the purified proteins, determined by chemical analysis, were identical to those that were expected from the genetic constructions, and they confirmed the presence of a His-tag. We experimentally determined the extinction coefficients at 280 nm for TyrRS−His6 (ϵ = 1.34 mL mg^{-1} cm^{-1}), its N-terminal fragment TyrRS(Δ1) (ϵ = 1.64 mL mg^{-1} cm^{-1}), and its C-terminal fragment TyrRS(Δ4) (ϵ = 0.46 mL mg^{-1} cm^{-1}), as described in the Materials and Methods section. Our values of these extinction coefficients differed significantly from those predicted from the sequences, 1.05, 1.28, and 0.50 mL mg^{-1} cm^{-1}, respectively (*20*), but were consistent with that previously determined for the wild-type TyrRS (ϵ = 1.3 mL mg^{-1} cm^{-1}) (*21*).

Analysis of the purified TyrRS−His6 by MALDI-TOF mass spectrometry gave a peak at 48 350.6 amu, a value which was close to its predicted M_r, 48 367. The purified TyrRS(Δ4) gave a major molecular ion at 11 980.8 amu with an internal calibration, and at 11 982.5 amu with an external calibration (Figure 3). These values were also close to the predicted M_r, 11 980.4. The differences between the predicted and experimental M_r were within the accuracy limits of MALDI-TOF mass spectrometry in linear mode. This analysis confirmed that the initiator methionine of TyrRS(Δ4) was excised in vivo by methionine aminopeptidase, as observed in *E. coli* for proteins whose second residue has a small radius of gyration (*22*).

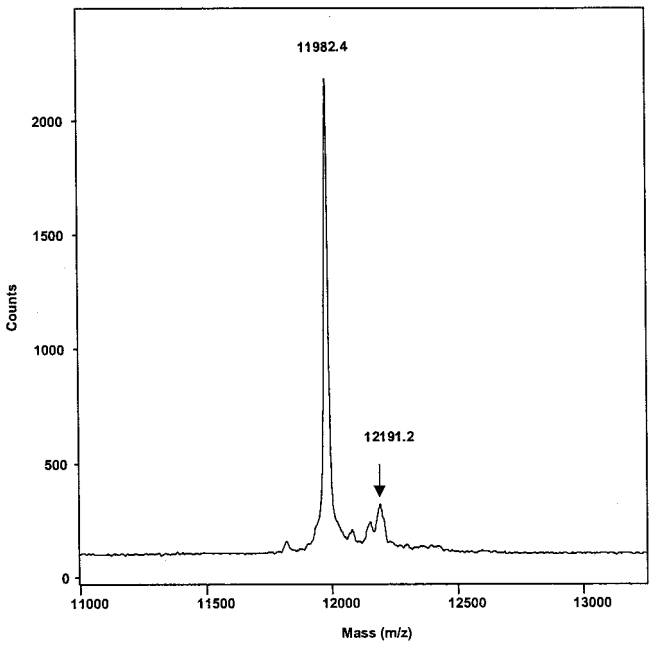

FIGURE 3: Analysis of the purified TyrRS(Δ4) by mass spectrometry, with external calibration. The major peak at 11 982.4 amu corresponds to TyrRS(Δ4). The minor peak at 12 191.2 amu corresponds to a matrix adduct produced during the analysis.

Enzymatic Properties of TyrRS−His6. We determined the kinetic parameters of the purified TyrRS−His6 hybrid protein for the charging of $tRNA^{Tyr}$, to test whether its His-tag perturbed the folding and activity of its TyrRS portion. The steady-state kinetic parameters for the aminoacylation of pure *E. coli* $tRNA^{Tyr}$ with tyrosine were $K_M(tRNA^{Tyr})$ = 1.8 ± 0.6 μM, k_{cat} = 6.3 ± 1.4 s^{-1}, and k_{cat}/K_M = 3.9 ± 0.6 $\mu M^{-1}\cdot s^{-1}$. The kinetic parameters of the native TyrRS, without a His-tag, are $K_M(tRNA^{Tyr})$ = 1.4 ± 0.2 μM, k_{cat} = 3.6 ± 0.3 s^{-1}, and k_{cat}/K_M= 2.7 ± 0.2 $\mu M^{-1}\cdot s^{-1}$ (*12*). Thus, the fusion with the His-tag did not affect the activity and hence the folding of TyrRS. Because the C-terminal domain is necessary for the binding of $tRNA^{Tyr}$ by TyrRS and thus involved in the catalytic reaction, we concluded that the folding and function of this domain were not affected by the His-tag in the full-length TyrRS−His6. No method for measuring the association between the C-terminal fragment of TyrRS and $tRNA^{Tyr}$ has been described so far. This association is probably weak, since mutation R207Q in the N-terminal domain of the full-length TyrRS decreases $K_M(tRNA^{Tyr})$ by more than 100-fold (*23*). Therefore, it was not possible to check the functional integrity of TyrRS(Δ4) directly.

Monomeric Behavior of the C-terminal Fragment. We characterized the oligomerization state of the C-terminal fragment TyrRS(Δ4) for two reasons. The contribution of the C-terminal domain to the dimerization of TyrRS has never been tested formally. Incompletely folded proteins, and in particular molten globules, are prone to aggregation (*24*, *25*). We performed this characterization by analytical ultracentrifugation. We did not find any evidence for aggregation during the approach to the equilibrium of sedimentation−diffusion. Moreover, we did not observe any evolution of

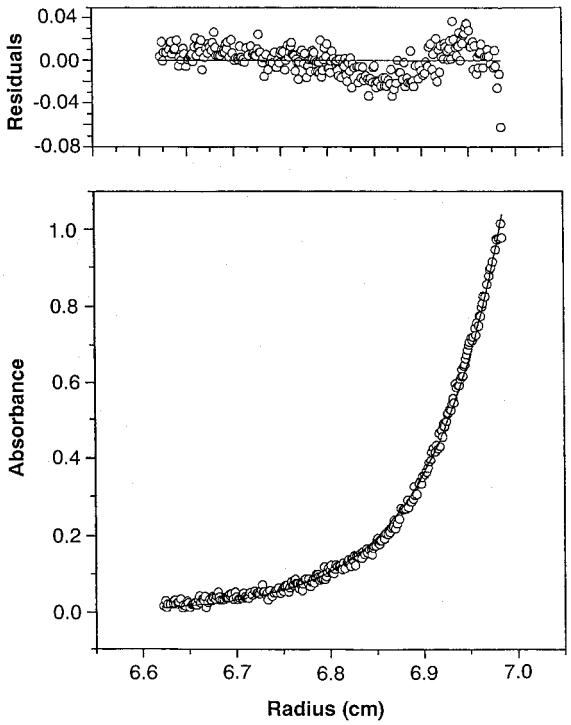

FIGURE 4: Equilibrium of sedimentation−diffusion for TyrRS(Δ4). The absorbance at 280 nm was scanned as a function of the distance to the axis of rotation of the analytical centrifuge. Lower panel: a theoretical curve (continuous line), corresponding to an ideal solution with one solute molecule, was fitted to the experimental points. Upper panel: plot of the residuals (difference between the experimental and theoretical values). See Materials and Methods for details.

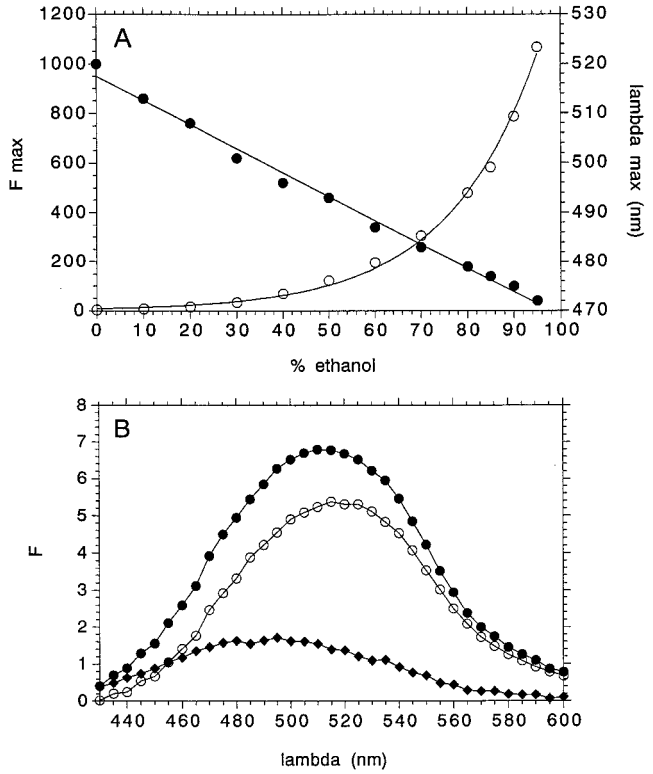

FIGURE 5: Binding of ANS to TyrRS(Δ4). The fluorescence of ANS was excited at 370 nm. (a) Fluorescence of ANS in a mixture of ethanol and water. The concentration of ANS was 0.1 mM. The figure gives the maximal intensity of fluorescence emission for ANS (○) and the corresponding wavelength (●) as a function of the composition of the ethanol/water mixture. Exponential and linear functions were fitted to the experimental data, respectively. (b) Spectra of fluorescence emission for ANS (0.1 mM) with (●) and without (○) TyrRS(Δ4) (4 μM) in buffer B, and the difference spectrum (◆). The fluorescence intensities, F_{max} and F, are on the same scale in (a) and (b).

the protein profile after the equilibrium was reached. These observations indicated that TyrRS(Δ4) did not aggregate, even slowly. We analyzed the protein distribution in the centrifugation cell at equilibrium, using different theoretical models (Materials and Methods). The equation that corresponded to an ideal solution with one solute molecule, gave a satisfactory fit to the measured A_{280nm}, according to the value of the statistical parameter χ^2 and to the random distribution of the residual values (Figure 4). The M_r obtained by this procedure was equal to 11 995 ± 187, and thus close to the predicted value for the TyrRS(Δ4) monomer, 11 980.4. Thus, TyrRS(Δ4) remained monomeric.

Stokes Radius of the C-terminal Fragment. The Stokes radius (R_S) of a polypeptide can be used as a measure of its compactness. It can be estimated by size-exclusion chromatography, by comparing the partition coefficient of the polypeptide under study to those of standard proteins (*14*, *15*). Using this approach (Materials and Methods), we found that the R_S value was equal to 21 ± 1 Å for the C-terminal fragment TyrRS(Δ4). This value can be compared with those for other polypeptide chains having about the same length (107 residues): 19 Å for the native thioredoxine of *E. coli* (108 residues); 19.3 Å for the native state of bovine pancreatic ribonuclease A (124 residues) and 32.8 Å for its denatured state (*14*); 24 Å for the F2 fragment of *E. coli* tryptophan synthase, a premolten globule (101 residues) (*7*). Thus, the R_S value for TyrRS(Δ4) showed a condensed state of folding.

Binding of ANS to the C-terminal Domain. The semiflexible nature of the molten globular state permits some internal nonpolar groups to become exposed to water, thus making the surface of this state more hydrophobic than those of the native and unfolded states. As a result, the molten globular state binds nonpolar molecules, like ANS, much more strongly than the two other states (*6*, *26*). We studied the binding of ANS, a small fluorescent hydrophobic molecule, to the C-terminal fragment TyrRS(Δ4). The fluorescence of ANS is very sensitive to its microenvironment. The quantum yield of the light emitted by ANS and the wavelength of its maximum are equal to 0.004 and 515 nm, respectively, in water, whereas the corresponding values are equal to 0.37 and 468 nm in 100% ethanol (*16*). We found that ANS had its maximum of fluorescence emission at the same wavelength, 495 nm, in the presence of TyrRS(Δ4) as in a mixture (46:54, v/v) of ethanol and water (Figure 5). By comparing the maximal intensity of the light that was emitted by 100 μM ANS in the presence of either 46% ethanol (Figure 5a) or 4 μM TyrRS(Δ4) (Figure 5b), we deduced that the concentration of ANS bound to TyrRS(Δ4) was equal to 2.33 μM and corresponded to 0.58 mole of ANS per mole of TyrRS(Δ4). The maximum intensity of fluorescence emission by ANS, bound to TyrRS(Δ4), was at a much higher wavelength than those for premolten or molten globules (see Discussion). These results showed that the solvent accessible surface of TyrRS(Δ4) was more hydrophilic than that of a molten globule.

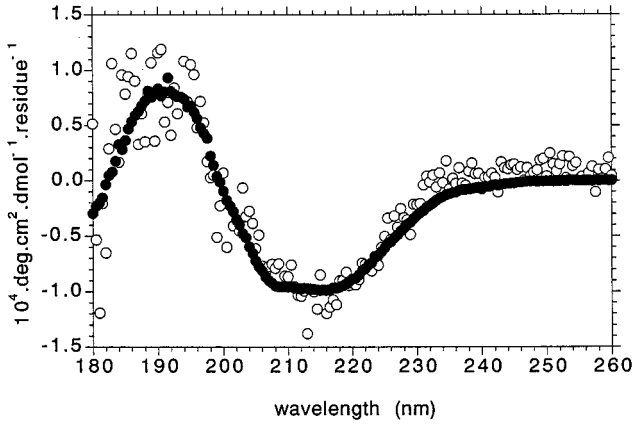

FIGURE 6: Circular dichroism spectrum of TyrRS(Δ4) at 25 °C in the far-UV region. (●) TyrRS(Δ4) was at 0.151 mM in buffer B, and the sample cell had a 0.1 mm optical path-length. The solvent contribution was subtracted from the sample spectrum. (○) Spectrum of TyrRS(Δ4), reconstructed by difference between those for TyrRS−His6 and TyrRS(Δ1).

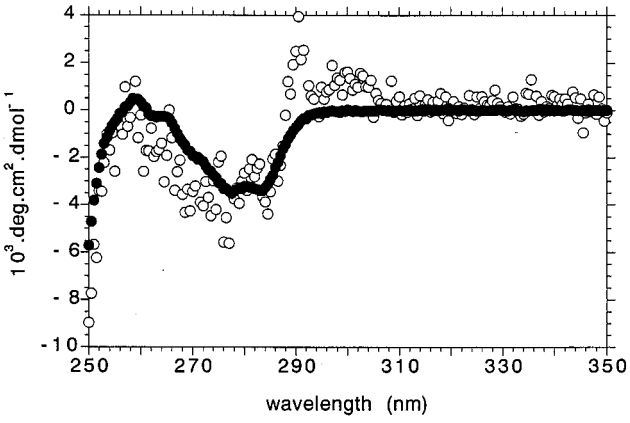

FIGURE 7: CD spectrum of TyrRS(Δ4) at 25 °C in the near-UV region. (●) TyrRS(Δ4) was at 0.156 mM in buffer B and the sample cell had a 1 cm path-length. The solvent contribution was subtracted from the sample spectrum. (○) Spectrum of TyrRS(Δ4), reconstructed by difference between those for TyrRS−His6 and TyrRS(Δ1).

Structural Analysis of the C-terminal Domain by Circular Dichroism. Typically, the far-UV CD spectra of proteins in the molten globular state are similar to those in the native state. This similarity indicates that a large proportion of the protein residues belong to secondary structure elements in the molten globular state. In contrast, the near-UV spectra are dramatically reduced in the molten globular state, as compared with the native state. This reduction in the spectra indicates an increased mobility of the side chains and a lack of rigid tertiary structure in the molten globular state (*6*). We recorded the CD spectra of the C-terminal fragment TyrRS(Δ4) in the far- and in the near-UV regions to test whether it is in a molten globular state. The CD spectrum in the far-UV (180−260 nm) showed a positive maximum around 195 nm and two negative minima at 207 and 217 nm, compatible with high proportions of residues in both α-helices and β-strands (Figure 6). A decomposition of this spectrum provided the following predictions for its content in secondary structures: 20% of residues in α-helices, 23% in antiparallel β-sheets, 8% in parallel β-sheets, and 20% in turns. The spectra in the far-UV and the decomposition in secondary structures were close for the two versions of the C-terminal fragment that we used, i.e., TyrRS(Δ4) which comprises a His-tag and TyrRS(Δ3) which does not comprise one (*4*). This comparison showed further that the His-tag did not perturb the folding of the protein.

The CD spectrum of TyrRS(Δ4) in the near-UV region showed marked maxima and minima (Figure 7). These characteristics indicated that the side chains of its aromatic residues (four Phe and four Tyr) were immobilized in asymmetric environments. They are typical for the stable tertiary structure of globular proteins (*6*, *25*, *27*−*29*). Thus, the CD spectra of TyrRS(Δ4) were compatible with a defined three-dimensional structure and not with a molten globular state.

To test whether the C-terminal domain possessed similar or different structures when it was integrated into its native protein context or isolated, we compared the CD spectra of the C-terminal fragment TyrRS(Δ4) with the difference between those for the full-length enzyme TyrRS−His6 and for its N-terminal fragment TyrRS(Δ1) (Figures 6 and 7). We found that a linear combination of the spectra for TyrRS−His6 and TyrRS(Δ1) could reproduce the spectrum for TyrRS(Δ4), both in the near-UV and in the far-UV regions. These comparisons strongly suggested that the C-terminal domain had similar contents in secondary structures and similar environments of its aromatic residues in its integrated and isolated forms. The rough aspect of the reconstructed spectra came from the cumulation of the errors on the two spectra and the much smaller number of residues in TyrRS(Δ4) (107 residues) when compared with TyrRS−His6 (427 residues) and TyrRS(Δ1) (319 residues).

DISCUSSION

The C-terminal domain of TyrRS has been described as disordered in its crystal structure and it is used as a prototype to predict the disordered segments of proteins from their sequences. We have shown recently that a recombinant version, TyrRS(Δ3), of the isolated C-terminal domain is not in a random coil conformation (see Introduction). However, the amounts of TyrRS(Δ3) that we could produce and purify were insufficient to characterize its folding state in detail. We solved this difficulty by constructing a strain of *E. coli* that overproduced a hybrid, TyrRS(Δ4), between the C-terminal fragment and a His-tag. We provided two pieces of evidence that the His-tag did not modify the folding of the C-terminal domain. The native TyrRS and the TyrRS−His6 hybrid, from which TyrRS(Δ3) and TyrRS(Δ4) derived respectively, had nearly identical steady-state kinetic parameters for the charging of $tRNA^{Tyr}$ with tyrosine. The CD spectra of TyrRS(Δ3) and TyrRS(Δ4) in the far-UV region were nearly identical. In the following paragraphs, we review the data and results in favor of a defined tertiary structure for the C-terminal domain and in disfavor of an intermediate state of folding, like the molten globular state. We then discuss the probable cause of its crystallographic disorder.

Evidence for a Defined Three-dimensional Structure. We have shown in a previous work that the C-terminal fragment TyrRS(Δ3) goes from a state where its tyrosine residues fluoresce strongly to a state where they fluoresce weakly in experiments of reversible denaturation by increasing concentrations of urea. TyrRS(Δ3) goes from a state of high mobility to a state of reduced mobility in experiments of electrophoresis across a transverse urea gradient. TyrRS(Δ3)

goes irreversibly from a soluble state to an insoluble state when it is heated at high temperatures. All these experiments have shown that TyrRS(Δ3) undergoes cooperative transitions that change its conformational state. The CD spectrum of TyrRS(Δ3) in the far-UV region has shown that a high proportion of its residues (around 70%) belong to elements of defined secondary structure. From these preliminary experiments, we have concluded that the C-terminal fragment is at least partially folded. We have determined that its conformational stability $\Delta G(H_2O)$ is equal to 4.3 ± 0.4 kcal/mol and its coefficient of cooperativity equal to 0.65 ± 0.08 kcal mol^{-1} M^{-1} at 25 °C in experiments of denaturation by urea (*4*, *30*).

In the present study, we measured the Stokes radius of a new version of the C-terminal fragment, TyrRS(Δ4), and compared its value, 21 Å, to those for proteins of similar molecular mass. This comparison indicated that TyrRS(Δ4) was in a condensed state of folding. Experiments of analytical centrifugation showed that TyrRS(Δ4) behaved as a monomer between 7.5 and 150 μM, i.e., its range of concentration in the cell of the centrifuge during the equilibrium of sedimentation−diffusion. This result showed that TyrRS(Δ4) remained monomeric at high concentrations and encouraged us to undertake its study by NMR (see below).

Three different methods have shown a high content in elements of secondary structure for the C-terminal fragment and an α+β type of fold. The decomposition of the CD spectrum of TyrRS(Δ4) in the far-UV region predicted that 20% of its residues belonged to α-helices, 31% to β-sheets (23% antiparallel and 8% parallel), and 20% to turns (this work). Eleven sequences of TyrRSs from prokaryotic or mitochondrial origins could be aligned and the alignment was submitted to five different algorithms of secondary-structure prediction from the sequence. The consensus of prediction contains 28% of residues in α-helices and 17% in β-sheets (*31*). Finally, a preliminary study of TyRS(Δ4) by NMR has shown that 25% of its residues are in α-helices and 19% in β-sheets (*32*). In this study by NMR, TyrRS(Δ4) was produced in *E. coli* and purified according to the procedure that we describe in the present report. Thus, three methods gave close estimates of the content in α-helical residues. As frequently observed, the content in β-sheet residues was less reliable than the content in α-helix residues when they were predicted from the CD spectrum (*18*).

The CD spectrum of TyrRS(Δ4) in the near-UV region contained marked maxima and minima of ellipticity. These properties showed that the aromatic residues of TyrRS(Δ4) were immobilized in asymmetrical environments, as a result of stable intramolecular contacts. They indicated the existence of a defined and stable tertiary structure. This conclusion is strengthened by an ongoing NMR study on TyrRS(Δ4) (unpublished data).

Evidence Against a Molten Globular State. The amount of stable secondary structure that can be detected in molten globules by NMR is limited and much smaller than the amount that is predicted from the CD spectrum in the far-UV region (*6*, *33*). The contents in secondary structures, estimated from the CD and NMR spectra, were in agreement, which suggested that the conformation of the C-terminal fragment TyrRS(Δ4) was less dynamic than a molten globule one. This conclusion was strengthened by the characteristics of its CD spectrum in the near-UV region (see above).

We found that ANS had its maximum of fluorescence emission at the same wavelength, 495 nm, when bound to TyrRS(Δ4) as when dissolved in a mixture (46:54, v/v) of ethanol/water. Therefore, ANS is bound to a partially hydrophilic region of TyrRS(Δ4). The emission maxima of ANS, bound to TyrRS(Δ4) (495 nm; this work), to a polylysine in a β-sheet conformation (500 nm) (*26*) and to the native hen egg lysozyme (500 nm) (*29*) had closely similar wavelengths. In contrast, the maxima of ANS bound to the F2 fragment of the *E. coli* tryptophan synthase, a premolten globule (474 nm) (*34*), and to the molten globular forms of carbonic anhydrase, α-lactalbumin, β-lactamase (about 470 nm) (*26*), and lysozyme in 25% TFA (478 nm) (*29*) had much lower wavelengths. Thus, the solvent accessible surface of TyrRS(Δ4) was more hydrophilic than a molten globule one.

Potential Causes of the Crystallographic Disorder. The N-terminal fragment TyrRS(Δ1) folds independently of the C-terminal domain: it has the same crystal structure as the N-terminal domain of the full-length TyrRS; it is dimeric as TyrRS and has a very high stability; it forms tyrosyl-adenylate normally (*30*, *35*, *36*). Reciprocally, our results showed that the C-terminal fragment TyrRS(Δ4) folded into a compact, stable, and defined structure, independently of the N-terminal domain of TyrRS. We found that the CD spectra of TyrRS(Δ4) in the near- and far-UV regions could be reconstructed by a difference between those of the full-length TyrRS−His6 and of its N-terminal fragment TyrRS(Δ1). This finding strongly suggested that the C-terminal fragment TyrRS(Δ4) had the same structure as the C-terminal domain of the full-length TyrRS, or a very similar one. Experiments of double hybrids, in which the N- and C-terminal fragments of TyrRS were the bait and the prey, did not reveal any interaction between them (*37;* G. Karimova et al., in preparation). All these data indicate that the N- and C-terminal domains do not form strong noncovalent tertiary interactions between them in the full-length TyrRS. Of course, a lack of detectable interaction between the two fragments as in the double hybrid experiments does not necessarily imply a lack of weak noncovalent tertiary interactions between the two corresponding domains, because their effective concentrations will be strongly increased by their covalent linkage in the full-length protein (*38*). The observation that the C-terminal domain is disordered in the crystal structure despite its defined structure, indicates that such weak interactions do not exist or that the N- and C-terminal domains can interact in several different ways between them. Thus, the available data indicate that the disorder of the C-terminal domain in the crystal structure results from the flexibility of the polypeptide segment that covalently links it to the N-terminal domain and suggest that the two domains may not interact together.

Comparison with Other Aminoacyl-tRNA Synthetases. The aminoacyl-tRNA synthetases (aaRS) are built in a modular way. Additional domains or modules are appended to the catalytic domain, which has an α/β-fold for the class I aaRSs and an antiparallel β-fold for the class II aaRSs. These additional domains have several functions: binding of the tRNA, editing, and multimerization. In the aaRSs of class IIa (ThrRS, HisRS, and GlyRS) and class IIb (AspRS, AsnRS, and LysRS), which are homodimeric, the anticodon-binding domain is connected to the catalytic domain through

a long extended peptide (*39*−*45*). The anticodon-binding domain of one subunit makes no or very few interactions with the catalytic domain of the same subunit, but it makes numerous interactions with the catalytic domain of the other subunit. In some structures, e.g. in HisRS and LysURS from *E. coli*, the connecting peptide has a high B-factor or is disordered, which suggests a high degree of conformational flexibility (*40*, *45*). In PheRS, which also belongs to class II and is an $\alpha_2\beta_2$ heterotetramer, the β subunit, which provides most of the tRNA-binding site, is composed of several domains that are separated by long extended segments. These domains do not interact with each other within the same subunit, but they make numerous interactions with the α-subunit, which contains the catalytic site, and with the β* subunit (*46*). Thus, contacts between subunits anchor the anticodon binding domain to the remainder of the molecule in the class II aaRSs.

The class I aaRSs are usually monomeric, except TyrRS and TrpRS, which are obligatory dimers. In MetRS, IleRS, and ArgRS, which belong to the same subclass, and in TrpRS, which belongs to a different subclass, the anticodon-binding domain is α-helical (*47*−*50*). The catalytic domain is followed by the anticodon-binding domain in the sequence, and numerous contacts exist between them in the structure. In MetRS, TrpRS, and perhaps IleRS (*51*), the anticodon-binding domain is followed by a C-terminal segment, which comes back toward the catalytic domain and staples the two domains together. In GlnRS, the catalytic domain (residues 1−348) is followed by two β-barrel domains, the distal domain (residues 348−464) then the proximal domain (residues 464−547) (*52*). In GluRS, the catalytic domain (residues 1−322) is followed by two α-helical domains, the proximal domain (residues 323−370), then the distal domain (residues 371−468) (*53*). In both cases, the proximal domain is inserted between the catalytic domain and the distal domain and gives its cohesion to the enzyme; the anticodon of the tRNA binds to a cleft between the proximal and distal domains (*54*, *55*). Thus, the anticodon-binding domain is firmly anchored to the catalytic domain for most class I aaRSs.

The N-terminal domain of TyrRS from *B. stearothermophilus* can be divided into two topological subdomains, an α/β subdomain (residues 1−220) containing a six-stranded β-sheet, followed by an α-helical subdomain (residues 248−318) containing five α-helices. These two subdomains make numerous contacts between them (*1*). Our results showed that the C-terminal domain (residues 320−419), which recognizes the anticodon arm of $tRNA^{Tyr}$, has a defined structure and that it is linked to the α-helical subdomain by a flexible connecting peptide. Thus, the above analysis of the aaRSs topologies and its comparison with our results show that TyrRS resembles many other aaRSs, in that its anticodon-binding domain has a defined structure and is linked to the remainder of the molecule by a flexible peptide. They show that TyrRS is an exception among the aaRSs, in that it has not evolved strong stabilizing tertiary interactions between its anticodon binding domain and the remainder of the molecule, neither within the same subunit as the other class I aaRSs, nor with the other subunit as the class II aaRSs.

The apparent disorder of the C-terminal domain of *B. stearothermophilus* TyrRS could have the same cause as the disorders of the N-terminal α-helical arms of SerRS and PheRS from *Thermus thermophilus*, which stretch out into the solvent and bind the extra-loop of $tRNA^{Ser}$ and the anticodon stem of $tRNA^{Phe}$. In the crystal structure of the free SerRS, the orientation of the helical arm (residues 24−100) with respect to the catalytic domain is different in the two subunits of the dimer (*56*). Moreover, in the structure of the 1:1 complex between SerRS and $tRNA^{Ser}$, the helical arm that interacts with the tRNA shows a third orientation, and the one that does not interact with the tRNA is partially absent (residues 34−86) from the electron density (*57*). Residues 1−84 of the α-subunit of PheRS are absent from the electron density of the free enzyme, whereas they form a helical arm, similar to the SerRS one, in the structure of the complex with $tRNA^{Phe}$ (*46*, *58*).

Comparison with Other TyrRSs and RNA-binding Proteins. In a previous work, we have shown that it is possible to align the sequences of the C-terminal domains of the prokaryotic and mitochondrial TyrRSs. In particular, the six basic residues of the C-terminal domain of TyrRS from *B. stearothermophilus* that are involved in the binding of the anticodon arm of $tRNA^{Tyr}$ and have been identified by mutagenesis are conserved between these TyrRSs. Moreover, the secondary structures of these C-terminal domains, predicted from their sequences, have a consensus that is close to the secondary structure of TyrRS from *B. stearothermophilus*, determined by NMR (*23*, *31*, *32*). These data of alignment and prediction suggest that the C-terminal domains of the other prokaryotic and mitochondrial TyrRSs, also reach a defined, stable, and independent structure.

Our results showed that the C-terminal fragment of TyrRS folded independently of the binding of $tRNA^{Tyr}$. Thus, the anticodon arm of $tRNA^{Tyr}$ binds to a structured C-terminal domain and does not induce its folding, as some other nucleic acids do for their binding proteins (*59*). However, in the hypothesis where the N- and C-terminal domains of TyrRS are linked covalently by a flexible polypeptide segment, the binding of $tRNA^{Tyr}$ may fix the respective orientations of the two domains in the complex.

Sequence homologies and residue identities have shown that the C-terminal domains of the prokaryotic TyrRSs belong to a numerous family of RNA-binding domains, the S4 family (*60*, *61*). Our results on the C-terminal domain of TyrRS from *B. stearothermophilus* suggest that the RNA-binding domains of the S4 family have a stable and defined structure in the absence of nucleic acid. The structure of the C-terminal fragment, determined by NMR, should provide the first three-dimensional model of this RNA-binding domain.

ACKNOWLEDGMENT

We thank M. Goldberg for helpful discussions, comments on the manuscript, and ultracentrifugation experiments; F. Baleux for the amino acid analyses; V. Redeker for the mass spectrometry experiments; Y. C. Park for purified TyrRS-(Δ1).

REFERENCES

1. Brick, P., Bhat, T. N., and Blow, D. M. (1989) *J. Mol. Biol. 208*, 83−98.
2. Dunker, A. K., Garner, E., Guillot, S., Romero, P., Albrecht, K., Hart, J., Obradovic, Z., Kissinger, C., and Villafranca, J. E. (1998) *Pacific Symposium on Biocomputing 1998*, pp 473−484.

3. Romero, P., Zoran, O., Kissinger, C. R., Villafranca, J. E., Garner, E., Guilliot, S., and Dunker, A. K. (1998) *Pacific Symposium on Biocomputing 1998*, pp 437−448.
4. Guez-Ivanier, V., and Bedouelle, H. (1996) *J. Mol. Biol. 234*, 209−221.
5. Fink, A. L. (1995) *Annu. Rev. Biophys. Biomol. Struct. 24*, 495−522.
6. Ptitsyn, O. B. (1995) *Adv. Protein Chem. 47*, 83−229.
7. Chaffotte, A. F., Guijarro, J. I., Guillou, Y., Delepierre, M., and Goldberg, M. E. (1997) *J. Protein Chem. 16*, 433−439.
8. Sambrook, J., Fritsch, E. F., and Maniatis, T. (1989) *Molecular cloning: a laboratory manual*, Cold Spring Harbor Laboratory Press, Cold Spring Harbor, N. Y.
9. Bedouelle, H., and Duplay, P. (1988) *Eur. J. Biochem. 171*, 541−549.
10. Bedouelle, H., Guez, V., Vidal-Cros, A., and Hermann, M. (1990) *J. Bacteriol. 172*, 3940−3943.
11. Guez-Ivanier, V., Hermann, M., Baldwin, D., and Bedouelle, H. (1993) *J. Mol. Biol. 234*, 209−221.
12. Vidal-Cros, A., and Bedouelle, H. (1992) *J. Mol. Biol. 223*, 801−810.
13. Tabor, S., and Richardson, C. C. (1987) *Proc. Natl. Acad. Sci. U.S.A. 84*, 4767−4771.
14. Corbett, R. J. T., and Roche, R. S. (1984) *Biochemistry 23*, 1888−1894.
15. Uversky, V. N. (1993) *Biochemistry 32*, 13288−13298.
16. Stryer, L. (1965) *J. Mol. Biol. 13*, 482−495.
17. Manavalan, P., and Johnson, Jr (1987) *Anal. Biochem. 167*, 76−85.
18. Johnson, Jr, W. C. (1990) *Proteins 7*, 205−214.
19. Studier, W., Rosenberg, A. H., Dunn, J. J., and Dubendorff, J. W. (1990) *Methods Enzymol. 185*, 61−85.
20. Pace, C. N., Vajdos, F., Fee, L., Grimsley, G., and Gray, T. (1995) *Protein Sci. 4*, 2411−2423.
21. Koch, G. L. (1974) *Biochemistry 13*, 2307−2312.
22. Hirel, P.-H, Schmitter, J.-M., Dessen, P., Fayat, G., and Blanquet, S. (1989) *Proc. Natl. Acad. Sci. U.S.A. 86*, 8247−8251.
23. Bedouelle, H., and Winter, G. (1986) *Nature 320*, 371−373.
24. O'Brien-Gress, J., Marquis-Omer, D., Middaugh, C. R., and Sanyal, G. (1994) *Biochemistry 33*, 2620−2627.
25. Kuwajima, K. (1989) *Proteins 6*, 87−103.
26. Semisotnov, G. V., Rodionova, N. A., Razgulyaev, O. I., Uversky, V. N., Gripas, A. F., and Gilmanshin, R. I. (1991) *Biopolymer 31*, 119−128.
27. Uversky, V. N., and Ptitsyn, O. B. (1996) *J. Mol. Biol. 255*, 215−228.
28. Schmid, F. X. (1997) in *Protein structure, a practical approach* (Creighton T. E., Ed.) 2nd edition, pp 261−297, Oxford University Press, Oxford.
29. Bhattacharjya, S., and Balaram, P. (1997) *Protein Sci. 6*, 1065−1073.
30. Park, Y. C., and Bedouelle, H. (1998) *J. Biol. Chem. 273*, 18052−18059.
31. Jermutus, L., Guez, V., and Bedouelle, H. (1999) *Biochimie 81*, 235−244.
32. Pintar, A., Guez, V., Castagne, C., Bedouelle, H., and Delepierre, M. (1999) *FEBS Lett. 446*, 81−85.
33. Dobson, C. M. (1994) *Current Biol. 4*, 636−640.
34. Chaffotte, A. F., Cadieux, C., Guillou, Y., and Goldberg, M. E. (1992) *Biochemistry 31*, 4303−4308.
35. Brick, P., and Blow, D. M. (1987) *J. Mol. Biol. 194*, 287−297.
36. Waye, M. M., Winter, G., Wilkinson, A. J., and Fersht, A. R. (1983) *EMBO J. 2*, 1827−1829.
37. Karimova, G., Pidoux, J., Ullmann, A., and Ladant, D. (1998) *Proc. Natl. Acad. Sci. U.S.A. 95*, 5752−9576.
38. Creighton, T. E. (1993) *Proteins, structure and molecular properties* 2nd edition, pp 163−165, W. H. Freeman and Company, New York.
39. Sankaranarayanan, R., Dock-Bregeon, A. C., Romby, P., Caillet, J., Springer, M., Rees, B., Ehresmann, C., Ehresmann, B., and Moras, D. (1999) *Cell 97*, 371−381.
40. Arnez, J. G., Harris, D. C., Mitschler, A., Rees, B., Francklyn, C. S., and Moras, D. (1995) *EMBO J. 14*, 4143−4155.
41. Logan, D. T., Mazauric, M. H., Kern, D., and Moras, D. (1995) *EMBO J. 14*, 4156−4167.
42. Cavarelli, J., Rees, B., Ruff, M., Thierry, J. C., and Moras, D. (1993) *Nature 362*, 181−184.
43. Berthet-Colominas, C., Seignovert, L., Hartlein, M., Grotli, M., Cusack, S., and Leberman, R. (1998) *EMBO J. 17*, 2947−2960.
44. Cusack, S., Yaremchuk, A., and Tukalo, M. (1996) *EMBO J. 15*, 6321−6334.
45. Onesti, S., Miller, A. D., and Brick, P. (1995) *Structure 3*, 163−176.
46. Goldgur, Y., Mosyak, L., Reshetnikova, L., Ankilova, V., Lavrik, O., Khodyreva, S., and Safro, M. (1997) *Structure 5*, 59−68.
47. Brunie, S., Zelwer, C., and Risler, J. L. (1990) *J. Mol. Biol. 216*, 411−424.
48. Nureki, O., Vassylyev, D. G., Tateno, M., Shimada, A., Nakama, T., Fukai, S., Konno, M., Hendrickson, T. L., Schimmel, P., and Yokoyama, S. (1998) *Science 280*, 578−582.
49. Cavarelli, J., Delagoutte, B., Eriani, G., Gangloff, J., and Moras, D. (1998) *EMBO J. 17*, 5438−5448.
50. Doublie, S., Bricogne, G., Gilmore, C., and Carter, C. W. Jr. (1995) *Structure 3*, 17−31.
51. Glasfeld, E., Landro, J. A., and Schimmel, P. (1996) *Biochemistry 35*, 4139−4145.
52. Rould, M. A., Perona, J. J., Soll, D., and Steitz, T. A. (1989) *Science 246*, 1135−1142.
53. Nureki, O., Vassylyev, D. G., Katayanagi, K., Shimizu, T., Sekine, S., Kigawa, T., Miyazawa, T., Yokoyama, S., and Morikawa, K. (1995) *Science 267*, 1958−1965.
54. Rould, M. A., Perona, J. J., and Steitz, T. A. (1991) *Nature 352*, 213−218.
55. Tateno, M., Nureki, O., Sekine, S., Kaneda, K., Go, M., and Yokoyama, S. (1995) *FEBS Lett. 377*, 77−81.
56. Fujinaga, M., Berthet-Colominas, C., Yaremchuk, A. D., Tukalo, M. A., and Cusack, S. (1993) *J. Mol. Biol. 234*, 222−233.
57. Biou, V., Yaremchuk, A., Tukalo, M., and Cusack, S. (1994) *J. Mol. Biol. 194*, 287−297.
58. Mosyak, L., Reshetnikova, L., Goldgur, Y., Delarue, M., and Safro, M. G. (1995) *Nat. Struct. Biol. 2*, 537−547.
59. Frankel, A. D. (1992) *Proc. Natl. Acad. Sci. U.S.A. 89*, 11653.
60. Aravind, L., and Koonin, E. V. (1999) *J. Mol. Evol. 48*, 291−302.
61. Korber, P., Zander, T., Herschlag, D., and Bardwell, J. C. (1999) *J. Biol. Chem. 274*, 249−256.
62. Winter, G., Koch, G. L., Hartley, B. S., and Barker, D. G. (1983) *Eur. J. Biochem. 132*, 383−387.
63. Waye, M. M., and Winter, G. (1986) *Eur. J. Biochem. 158*, 505−510.

BI992382V